

Magnetic order in acentric Pb_2MnO_4

Simon A. J. Kimber^{ab} and J. Paul Attfield^{*ab}

Received 22nd March 2007, Accepted 4th October 2007

First published as an Advance Article on the web 11th October 2007

DOI: 10.1039/b704361a

The low temperature magnetic properties of Pb_2MnO_4 , which crystallises in an acentric but non-polar space group ($P\bar{4}2_1c$) that allows piezoelectricity, have been investigated. Magnetisation measurements reveal a sharp transition to an antiferromagnetically ordered state at 18 K. Powder neutron diffraction at 1.5 K shows the spin structure to have a (000) propagation vector with Mn^{4+} moments of $2.74(2) \mu_B$ lying in the ab plane. The magnetic symmetry group is $P\bar{4}'2_1c'$ which permits piezomagnetism (stress-induced weak ferromagnetism). Possible ‘multipiezo’ properties of coupled magnetisation and electrical polarisation under mechanical stress in Pb_2MnO_4 are briefly discussed.

Introduction

Multiferroics are at the forefront of materials research^{1–3} as coupling between polarisation and magnetic degrees of freedom has the potential to provide new types of devices.⁴ Unfortunately the combination of ferroelectricity and ferromagnetism is rare^{5,6} and a large magnetoelectric effect requires both a large electric and a large magnetic susceptibility.⁷ Recently, several mechanisms that drive spontaneous polarisation in magnetic materials have been proposed, including electrostatic and size effects in YMnO_3 ,^{8–10} incommensurate magnetic order in the RMnO_3 ,^{11,12} and RMn_2O_5 ,^{13–16} (R = rare earth) materials and charge order in doped manganite perovskites.¹⁷ The symmetry requirements for improper ferroelectricity induced by spin order have also recently been formalised.¹⁸ An alternative and more practical route to magnetoelectrics is to use composite materials. These combine a magnetostrictive phase and a piezoelectric phase, for example, CoFe_2O_4 and BaTiO_3 . Applying a magnetic field yields large polarisation *via* internal stresses, up to several orders of magnitude higher than those shown in single phase magnetoelectric materials.¹⁹

The combination of piezoelectric and magnetic properties in a single phase is attractive, in particular for materials that crystallise in acentric but non-polar space groups. If antiferroelectric and antiferromagnetic, these materials can show stress-induced multiferroic properties of electrical and magnetic polarisation (piezo-electricity and -magnetism) and we thus label such materials as ‘multipiezoelectrics’. The magnitude of observable multipiezo effects is determined by the mechanical strength of a suitable material under appropriate uniaxial or shear stress and the components of the piezoelectric and piezomagnetic tensors.

Pb_2MnO_4 has previously been reported to crystallise in the acentric but non-polar space group ($P\bar{4}2_1c$)²⁰ which allows piezoelectricity.²¹ The structure (Fig. 1) consists of zigzag chains of edge-sharing MnO_6 octahedra parallel to the c axis

that delimit one-dimensional tunnels into which the Pb^{2+} cations project. These have an off-centre coordination by oxygen that may be attributed to a $6s^2$ electron lone pair. There are two types of tunnel in Pb_2MnO_4 ; the larger (*ca.* 4.3 Å diameter) is lined by $\text{Pb}(2)$ and is centred at $(1/2, 0, z)$ and the smaller tunnel (*ca.* 3.7 Å diameter) is lined by $\text{Pb}(1)$ and is centred on $(1/2, 1/2, z)$. As Pb_2MnO_4 also contains magnetic $3d^3 \text{Mn}^{4+}$ ions, it is likely that a long range ordered spin state is formed at low temperatures. We have determined this ordering by magnetisation and neutron diffraction measurements and we show that the magnetic (Shubnikov) symmetry is compatible with piezomagnetism, making Pb_2MnO_4 a candidate multipiezo material.

Experimental

Polycrystalline Pb_2MnO_4 was synthesised from PbO (99.999%, Aldrich) and Mn_2O_3 (99.999%, Aldrich). Stoichiometric quantities of the reagents were intimately ground, pelleted

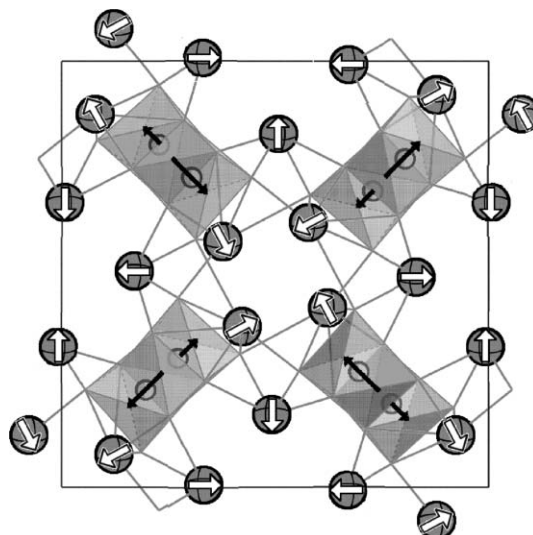


Fig. 1 [001] Projection of the crystal and magnetic structures of Pb_2MnO_4 , with Pb^{2+} electrical dipoles marked as white arrows and Mn^{4+} magnetic moments as black arrows. MnO_6 octahedra are shaded and $\text{Pb}-\text{O}$ bonds are shown as lines.

^aCentre for Science at Extreme Conditions, University of Edinburgh, Erskine-Williams Building, King's Buildings, Mayfield Road, Edinburgh, UK EH9 3JZ

^bSchool of Chemistry, University of Edinburgh, Joseph Black Building, King's Buildings, West Mains Road, Edinburgh, UK EH9 3JJ

and reacted under air for a total of one week at 730 °C with several intermediate regrinds. Phase purity was checked by powder X-ray diffraction. Electrical measurements showed that Pb_2MnO_4 is highly resistive ($>10^7 \Omega \text{ cm}$) at room temperature.

Magnetisation measurements were performed using a Quantum Design SQUID magnetometer under field (1 T) and zero-field cooled conditions. Time of flight neutron powder diffraction data were recorded using the instrument OSIRIS at the ISIS facility, UK. OSIRIS is a long wavelength diffractometer²² giving high $\Delta d/d$ resolution up to d -spacings of 25 Å. A 10 g sample of Pb_2MnO_4 was placed in a vanadium can and data were collected at 1.5 K for 20 h. The General Structure Analysis System²³ (GSAS) was used to fit the neutron diffraction profiles.

Results

Magnetisation

The magnetic susceptibility and inverse susceptibility data shown in Fig. 2 reveal a sharp transition to a three-dimensionally ordered antiferromagnetic state below $T_N = 18$ K. The inverse susceptibility follows a Curie–Weiss law with an observed paramagnetic moment of $3.88 \mu_B$, in excellent agreement with the predicted spin-only moment for Mn^{4+} ($3.87 \mu_B$). The Weiss constant is negative (-42.2 K) indicating dominant antiferromagnetic interactions between Mn^{4+} spins. No divergence between field and zero-field cooled measurements was observed, confirming that the ground state is antiferromagnetic with no spontaneous magnetisation.

Several attempts were made to detect a low temperature piezomagnetic response of Pb_2MnO_4 below T_N . A small sintered pellet was placed in a short Cu–Be pressure cell²⁴ between two zirconia pistons. A small piece of indium wire was placed between the sample and the top piston to calibrate pressure through variation of the superconducting transition

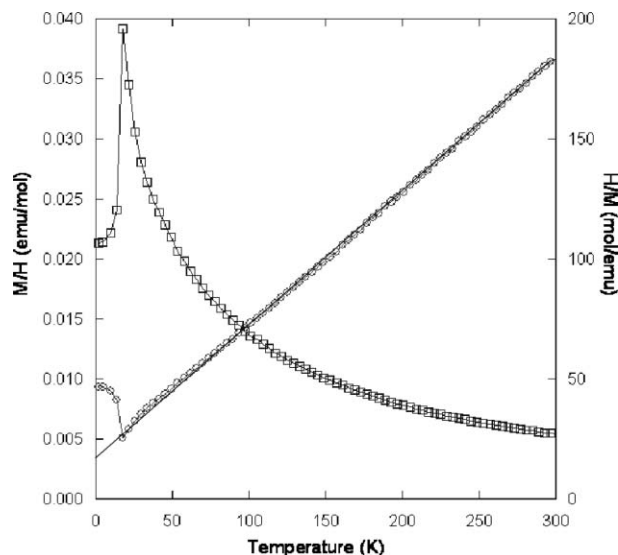


Fig. 2 Magnetic susceptibility (M/H) (□) and inverse susceptibility (○) of Pb_2MnO_4 as a function of temperature. The line shows a Curie–Weiss fit in the range 100–300 K, extrapolated to low temperatures.

temperature. However, the ceramic pellets always cracked or broke under applied stress and so no reliable piezomagnetic response was observed.

Neutron diffraction

No distortion from tetragonal symmetry was apparent in the 1.5 K neutron data (Fig. 3), so these were fitted using the previously reported room temperature structural model in space group $P\bar{4}2_1c$.²⁰ The diffraction peak shape was modelled with a convolution of an Ikeda–Carpenter and a pseudo-Voigt function²⁵ and the background was fitted by a linear interpolation function.

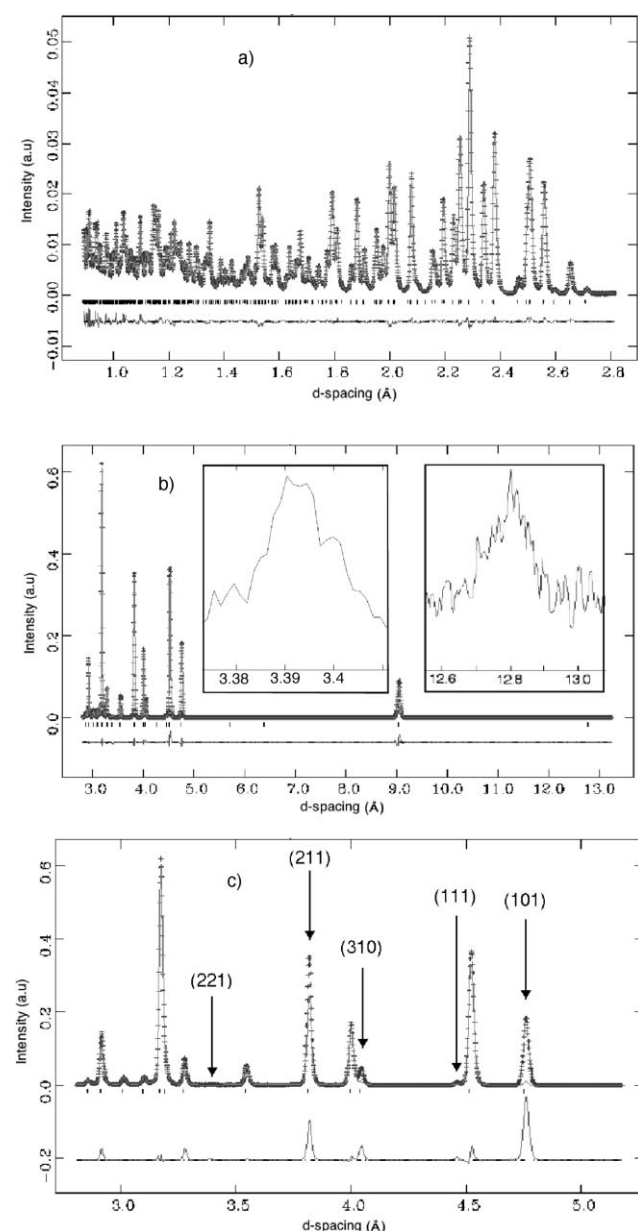


Fig. 3 Observed, calculated and difference plots for the Rietveld fit to the time-of-flight neutron diffraction profile of Pb_2MnO_4 : (a) and (b) display the final fit of the nuclear and magnetic structures; (c) shows a fit of only the nuclear structure with magnetic peaks labelled; the weak (221) and (100) magnetic peaks are shown in the insets to (b).

Table 1 Refined atomic coordinates and isotropic thermal U-parameters for Pb_2MnO_4 at 1.5 K in space group $\bar{P}42_1c$. The refined cell parameters are $a = 12.78027(10)$ Å and $c = 5.12418(6)$ Å

Atom	<i>x</i>	<i>y</i>	<i>z</i>	U_{iso} /Å ²
Pb(1)	0.07798(6)	0.12310(5)	0.2459(2)	0.0044(3)
Pb(2)	0.00754(5)	0.33043(6)	0.7940(1)	0.0027(1)
Mn	0.3072(1)	0.2706(1)	0.2572(5)	0.0014(6)
O(1)	0.3155(1)	0.4143(1)	0.1560(3)	0.0057(5)
O(2)	0.2802(1)	0.1405(1)	0.4355(3)	0.0050(5)
O(3)	0.3252(1)	0.7567(1)	0.4241(2)	0.0018(5)
O(4)	0.2703(1)	0.5581(1)	0.5993(3)	0.0067(5)

After fitting the contributions from the crystal structure, several peaks at high *d*-spacing showed extra intensity and three additional weak peaks were also evident (see Fig. 3b and c), at *d* = 3.39, 4.46 and 12.78 Å, corresponding respectively to the (221), (111) and (100) reflections. These are systematically absent from the $\bar{P}42_1c$ space group. No other magnetic peaks were seen, so several possible antiferromagnetic models were constructed with a (000) propagation vector. The possible Shubnikov groups are: $\bar{P}42_1c$, $\bar{P}4'2_1c$, $\bar{P}4'2_1c'$ and $\bar{P}42'_1c'$ (where the primed symbols have a time reversal symmetry operation) and only those having the $\bar{4}'$ operation generate the above weak peaks, which are systematically absent in the parent group symmetry. Only models having Shubnikov group symmetry $\bar{P}4'2_1c'$ gave a good fit to the intensities. The Mn^{4+} moments are oriented in $\langle 110 \rangle$ or $\langle -110 \rangle$ directions and are parallel to the *ab*-plane, as shown in Fig. 1. The final fit of the crystal and magnetic structures to the 1.5 K neutron data gave residuals $R_p = 3.49\%$ and $\text{w}R_p = 3.51\%$ and the results in Tables 1 and 2. These are in agreement with those previously reported for tetragonal Pb_2MnO_4 at 300 K,²⁰ but are more precise. The refined moment of 2.74(2) μ_{B} shows a typical reduction from the ideal value of 3 μ_{B} for Mn^{4+} due to covalency effects.

Discussion

The ionic contribution to the polarisability is large in oxides and the piezoelectric response of Pb_2MnO_4 will be dominated by dipoles that result from the off-centre cation displacements of Pb^{2+} ions. The inequivalent Pb(1) and Pb(2) sites are

Table 2 Selected bond distances (Å) and angles (deg.) for Pb_2MnO_4 at 1.5 K

Mn–O(1)	1.911(3)
Mn–O(2)	1.928(3), 1.893(4)
Mn–O(3)	1.955(3), 1.939(3)
Mn–O(4)	1.871(3)
$\langle \text{Mn}–\text{O} \rangle$	1.916(3)
Mn–O(2)–Mn	99.81(12)
Mn–O(3)–Mn	97.31(11)
Pb(1)–O(1)	2.245(2)
Pb(1)–O(2)	2.770(2)
Pb(1)–O(3)	2.282(2)
Pb(1)–O(4)	2.753(3), 2.333(2)
$\langle \text{Pb}–\text{O}(1) \rangle$	2.476(2)
Pb(2)–O(1)	2.231(2)
Pb(2)–O(2)	2.319(2)
Pb(2)–O(3)	2.746(2)
Pb(2)–O(4)	2.193(2)
$\langle \text{Pb}–\text{O}(2) \rangle$	2.372(2)

coordinated by five and four oxygens respectively. By calculating the centroids of the coordinating oxygens from the atomic coordinates in Table 1, the displacement vectors, *r*, of the Pb^{2+} cations away from the centres of their coordination environments are found to be $(-0.82, -0.65, -0.36)$ for Pb(1) and $(-0.10, 1.19, -0.26)$ for Pb(2), where components in Å units are parallel to *a*, *b* and *c*, and the vector magnitudes are 1.11 and 1.22 Å. The *r* vectors estimate the directions in which the Pb^{2+} lone pairs point and so correspond to the approximate directions of the local dipoles. These lie near-parallel to the *ab* plane in Pb_2MnO_4 , as illustrated in Fig. 1. The bulk induced polarisation *P_i* is related to the stress tensor *s_j* via the piezoelectric modulus *d_{ij}*: $\text{P}_i = d_{ij}\text{s}_j$. The crystal structure of Pb_2MnO_4 belongs to point group $\bar{4}2m$ and so the only non-zero piezoelectric coefficients are *d₁₄* and *d₃₆*.

The magnetic structure of Pb_2MnO_4 is illustrated in Fig. 1 and consists of antiferromagnetic chains with moments parallel to the *ab* plane, coupled antiparallel to those in the nearest neighbour chains. The intrachain Mn–O–Mn angles of 100 and 97° would be expected to lead to ferromagnetic superexchange,²⁶ but direct Mn–Mn exchange leads to antiferromagnetic interactions.²⁷ Weaker superexchange interactions²⁸ via Mn–O–Pb–O–Mn bridges lead to long range spin order. The Mn–Mn distance within the chains is 2.92 Å, whereas the shortest interchain Mn–Mn distance is 5.96 Å, so that some one-dimensional behaviour might be expected. However, the magnetic susceptibility (Fig. 3) shows that Pb_2MnO_4 behaves as a three-dimensional antiferromagnet with no short range correlations evident above the Néel transition at $T_N = 18$ K.

The stress-induced magnetisation *M_i* is described by an analogous equation to that above; $\text{M}_i = c_{ij}\text{s}_j$, where *c_{ij}* is the piezomagnetic tensor.²⁹ Piezomagnetism is less studied than piezoelectricity, but the *c_{ij}* components have been determined experimentally in crystals of the centrosymmetric fluorides CoF_2 and MnF_2 .³⁰ The spin arrangement determined for Pb_2MnO_4 is described by Shubnikov group $\bar{P}4'2_1c'$ and this has *c₁₄* and *c₃₆* as the only non-zero piezomagnetic coefficients.

The above symmetry and structural considerations show that Pb_2MnO_4 is a good candidate material for the investigation of multipiezo properties below the magnetic ordering temperature of 18 K. The acentric but non-polar crystal symmetry is unchanged down to 1.5 K, and the spin structure has a compatible symmetry, so that ferroelectricity and (weak) ferromagnetism are not permitted, but piezo-electricity and -magnetism are symmetry allowed. The electric dipoles from the Pb^{2+} displacements are approximately parallel to the *ab* plane in which the Mn^{4+} magnetic moments lie. This might give rise to significant coupling between the polarisation and magnetisation responses when tetragonal symmetry is broken by an applied shear stress. Converse piezoelectric or magnetostrictive effects in which application of an electric or magnetic field generates a strain should also be observable. Our initial attempts to observe a piezomagnetic response from sintered pellets of Pb_2MnO_4 were unsuccessful, and suitable single crystals or epitaxial films will be needed to measure such properties.

In summary, the acentric but non-polar material Pb_2MnO_4 is found to order antiferromagnetically below 18 K with

Shubnikov group symmetry $P\bar{4}'2_1c'$ and Mn⁴⁺ moments of $2.74\ \mu_B$ lying parallel to the ab plane. Electrical dipoles from off-centre Pb²⁺ displacements also lie close to this plane, and so significant stress-induced polarisations and magnetisations are anticipated. Pb₂MnO₄ may thus prove to be a multipiezoelectric material at low temperatures.

Acknowledgements

The authors thank the EPSRC for the provision of neutron beam time at ISIS and for a studentship for SAJK, and the Leverhulme Trust for support. We also thank Dr M. Telling (ISIS) and Dr L. Ortega-San Martin (UoE) for assistance with the neutron measurements, and Dr K. Kamenev and Dr J. Sanchez-Benitez for undertaking the piezomagnetism experiments.

References

- 1 M. Fiebig, *J. Phys. D: Appl. Phys.*, 2005, **38**, R123.
- 2 N. A. Spaldin and M. Fiebig, *Science*, 2005, **309**, 391.
- 3 W. Eerenstein, N. D. Mathur and J. F. Scott, *Nature*, 2006, **442**, 759.
- 4 V. E. Wood and A. E. Austin, *Int. J. Magn.*, 1973, **5**, 303.
- 5 N. A. Hill, *J. Phys. Chem. B*, 2000, **104**, 6694.
- 6 N. A. Hill, *J. Magn. Magn. Mater.*, 2002, **242**, 976.
- 7 W. F. Brown, R. M. Hornreich and S. Shtrikman, *Phys. Rev.*, 1968, **168**, 574.
- 8 Z. J. Huang, Y. Cao, Y. Y. Sun, Y. Y. Xue and C. W. Chu, *Phys. Rev. B*, 1997, **56**, 2623.
- 9 M. Fiebig, T. Lottermoser, D. Frohlich, A. V. Goitsev and R. V. Pisarev, *Nature*, 2002, **419**, 818.
- 10 B. B. Van Aken, T. T. M. Palstra, A. Filippetti and N. A. Spaldin, *Nat. Mater.*, 2004, **3**, 164.
- 11 T. Kimura, T. Goto, H. Shintani, K. Ishizaka, T. Arima and Y. Tokura, *Nature*, 2003, **426**, 55.
- 12 T. Goto, G. Lawes, A. P. Ramirez and Y. Tokura, *Phys. Rev. Lett.*, 2004, **92**, 257201.
- 13 N. Hur, S. Park, P. A. Sharma, J. S. Ahn, S. Guha and S. W. Cheong, *Nature*, 2004, **429**, 392.
- 14 L. C. Chapon, G. R. Blake, M. J. Gutman, S. Park, N. Hur, P. G. Radaelli and S. W. Cheong, *Phys. Rev. Lett.*, 2004, **93**, 177402.
- 15 G. R. Blake, L. C. Chapon, P. G. Radaelli, S. Park, N. Hur, S. W. Cheong and J. Rodriguez-Carvajal, *Phys. Rev. B*, 2005, **71**, 214402.
- 16 L. C. Chapon, P. G. Radaelli, G. R. Blake, S. Park and S. W. Cheong, *Phys. Rev. Lett.*, 2006, **96**, 097601.
- 17 D. V. Efremov, J. van den Brink and D. I. Khomskii, *Nat. Mater.*, 2004, **3**, 853.
- 18 P. G. Radaelli and L. C. Chapon, arXiv:cond-mat/0609087, 2006.
- 19 C. W. Nan, *Phys. Rev. B*, 1994, **50**, 6082.
- 20 A. Teichert and H. K. Muller-Buschbaum, *Z. Anorg. Allg. Chem.*, 1991, **598–599**, 319.
- 21 P. S. Halasyamani and K. R. Poeppelmeier, *Chem. Mater.*, 1998, **10**, 2753.
- 22 D. M. Y. Marero and D. Engberg, *Physica B*, 1999, **268**, 134.
- 23 A. C. Larson and R. B. von Dreele, Los Alamos National Laboratory Report, No. LAUR 86-748, 1994.
- 24 J. Kamarád, Z. Machátová and Z. Arnold, *Rev. Sci. Instrum.*, 2004, **75**, 5022.
- 25 W. I. F. David, *J. Appl. Crystallogr.*, 1986, **19**, 63.
- 26 J. B. Goodenough, *Magnetism and the Chemical Bond*, Interscience, New York, 1963.
- 27 J. B. Goodenough, *Phys. Rev.*, 1960, **117**, 1442.
- 28 J. M. Mays, *Phys. Rev.*, 1963, **38**, 131.
- 29 *International Tables for Crystallography: Volume D*, Kluwer Academic Publishers, Dordrecht, 2003.
- 30 A. S. Borovik-Romanov, *Sov. Phys. JETP (Engl. Transl.)*, 1960, **11**, 786.